

An environmentally friendly, biodegradable, antioxidant, and antibacterial food packaging made from polylactic acid, nano chitosan, and iron nanoparticles produced through green synthesis

Marzieh Piryaei^{1✉} | Mir Mehdi Abolghasemi² | Samira Azhdarifam² | Zahra Farhadi²

1. Department of Chemistry, University of Maragheh, Maragheh, Iran. Email: m.piryaei@gmail.com

2. Department of Chemistry, University of Maragheh, Maragheh, Iran.

Article Info

Article type:
Research Article

Keywords:
Biodegradable polymers,
green synthesis,
Antibacterial,
polylactic acid
chitosan

ABSTRACT

The increasing demand for sustainable and functional food packaging materials has stimulated research into biodegradable polymers reinforced with active compounds. This study addresses this need by developing a novel polylactic acid [1]-based film combined with green-method synthesized iron nanoparticles (using *Artemisia absinthium* extract) and nanochitosan to create an active packaging material with enhanced antibacterial and antioxidant properties. A biodegradable food packaging film was developed using polylactic acid, nanochitosan, and iron nanoparticles synthesized via a green-method using *Artemisia absinthium* (wormwood) extract. The main objective was to create a material with antibacterial and antioxidant properties to extend the shelf life of food products. Iron nanoparticles were synthesized using the extract and $\text{FeCl}_3 \cdot 6\text{H}_2\text{O}$ and then coated with chitosan. The films were produced by solvent casting and their properties were investigated. The results showed that the antibacterial and antioxidant capabilities were significantly improved by adding the extract and nanoparticles. The film containing 5% extract showed optimal flexibility and antibacterial performance. The DPPH radical scavenging activity increased with increasing extract concentration and the films showed strong inhibition against *S. aureus* and *E. coli*. The films had lower water vapor permeability, average thickness of 0.089 ± 0.01 cm, moisture content of $65.61 \pm 3.84\%$ and solubility of $18.09 \pm 2.51\%$ indicating good stability. SEM, FTIR and XRD confirmed the successful synthesis and incorporation of nanoparticles. The greenness of the method was evaluated using AGREEprep software and scored 0.8, indicating high environmental compatibility.

INTRODUCTION

The emergence of advanced technologies, including green nanotechnology, advanced materials and composites, and nanostructures, has revolutionized approaches to sustainability and environmental challenges, offering innovative solutions for remediation, wastewater treatment, renewable energy generation and storage, and overall improvement of human well-being. For example, green nanotechnology uses environmentally friendly synthesis methods to engineer nanomaterials that effectively adsorb pollutants from contaminated water sources and facilitate cost-effective environmental remediation while minimizing secondary ecological impacts. Advanced composites, such as carbon nanotube-reinforced polymers, enable the development of

lightweight and durable structures for solar panels and wind turbines, thereby increasing the efficiency of clean energy generation and storage systems, such as high-capacity batteries that incorporate nanostructured electrodes for improved charge-discharge cycles. These technologies generally address important environmental issues-such as mitigating climate change and resource depletion-by promoting circular economies, reducing greenhouse gas emissions, and ensuring access to clean water and energy, ultimately fostering resilient societies and improving quality of life through sustainable innovation[1-6].

Today, polymers and materials used in food packaging include a wide range of petroleum-based polymers, metals, paper, glass and wood or a combination of these materials. one of the most important applications of plastics since the

How to Cite this paper: Piryaei M. Abolghasemi M. M. Azhdarifam S. Farhadi Z. An environmentally friendly, biodegradable, antioxidant, and antibacterial food packaging made from polylactic acid, nano chitosan, and iron nanoparticles produced through green synthesis. *Challenges in Nano and Micro Scale Science and Technology*. 2025; 13(1): 15-28. DOI: 10.22111/cnmst.2026.54408.1275



end of the 20th century has been the use in the packaging industry, of which 47% is related to food packaging. Today, these packages are mostly polyolefins such as polypropylene, polyethylene, polyethylene terephthalate, polyvinyl chloride, etc., which are all sourced from fossil fuels. Low price, high production speed, high mechanical strength, good inhibition feature and good thermal sealing capabilities are advantages of petroleum-based polymers that encourage industries to use them [7, 8].

Of course, these types of packaging also have disadvantages such as the decline of oil and gas resources, rising oil and gas prices, environmental concerns about their non-degradation and global warming, low economic benefit and cross-contamination from their recycling and the risk of disease in the consumer due to the migration of toxic substances to food [7, 9].

According to the American Society for Testing and Materials Standards, biodegradable plastic refers to plastic that microorganisms like bacteria, fungi, and algae can break down. Compostable plastic, on the other hand, decomposes through biological processes to form carbon dioxide, water, inorganic compounds, biomass, and compost, without causing harmful effects. Therefore, the production and development of biodegradable polymer materials is a necessity for societies and therefore has provided a great interest in research on biodegradable materials with special properties for materials experts in the world. Biodegradable polymers are categorized into two primary types, with the first group being derived from natural renewable sources like polylactic acid, polyhydroxybutyrate and their copolymers, as well as starch, cellulose, gelatin, chitosan, and similar materials. The second group is sourced from oil sources [10-15].

Due to environmental and ecological attractions, biodegradable polymers that are made from natural renewable sources have attracted a lot of attention nowadays. The key applications of these materials include their capacity to biodegrade, minimize waste production, transform into fertilizers within natural cycles, lower carbon dioxide levels, and utilize agricultural resources to manufacture biodegradable polymers. [16]

Many biodegradable polymers have very good mechanical, and thermal properties that are comparable to petroleum-based plastics, but have limitations such as fragility and high permeability to gases.

So far, iron oxide is the most important ingredient in medicine due to its chemical stability and biological versatility, as well as the relatively simple production process of magnetite nanoparticles (Fe_3O_4) and maghemite ($\text{Fe}_2\text{O}_3\text{-}\gamma$). Mixtures of these two nanoparticles can be synthesized by deposition of Fe^{2+} and Fe^{3+} iron ions salts.

Practical experiments have shown that it is possible to recover iron oxide compounds from such mixtures naturally and orderly. Human body compounds such as proteins, ferritins, hemosiderins, transferritin and hemoglobin contain 3 to 4 grams of iron when magnetic nanoparticles are decomposed within the body, degrading iron enters the iron reservoirs in the body.

Chitosan polysaccharides that are extracted from the crustacean and insects in the form of chitin and then converted into chitosan. This polysaccharide is biodegradable and has a positive charge. Different conditions of chitosan extraction cause different molecular weights and different degrees of deacetylation (40%-98%).

Synthesis of nanoparticles using plant extracts called green synthesis is a new, very simple, economical and environmentally friendly method. Green synthesis and production of environmentally friendly materials is considered as an important scientific achievement in nanoscience. Microbial synthesis, as a method for biological production of nanoparticles, is unsuitable for industrial applications due to harsh storage conditions and the need for a highly sterile and disinfected environment. Microorganisms, especially bacteria, can also be used to produce nanoparticles, but due to the low speed and limited size of nanoparticles, they are less efficient than other green synthesis methods based on plants. In addition, fungi and bacteria require a lot of time to reduce iron ions, while water-soluble plant chemical compounds do so in much less time. Of these plants, the best and most suitable method for synthesis of nanoparticles mainly and allows for a certain size and form of synthesis. The production of biocompatible nanoparticles through green synthesis methods, which avoids the use of chemicals, has gained attention. Utilizing organisms to produce metal nanoparticles is one of the key approaches in green synthesis. Additionally, employing different plant materials for nanoparticle synthesis is regarded as a green technology because it excludes harmful chemicals [17].

Magnetic nanoparticles have numerous applications in water and wastewater treatment and are of great environmental importance. The use of magnetic nanoparticles as effective adsorbents for the removal of pollutants, especially heavy metals and organic compounds, helps reduce water pollution. These nanoparticles can reduce up to 99% of water pollutants, which helps improve water quality and protect water resources. Also, the synthesis of magnetic nanoparticles using green methods, such as extracting plant extracts, helps reduce negative environmental impacts. These methods use natural resources instead of using harmful chemicals, and as a result, produce less pollution. In addition, magnetic nanoparticles are known as more sustainable options for water treatment due to their easy recovery using a magnetic field. This feature helps reduce costs and consumption of natural resources, and leads to sustainable management of water resources. Ultimately, magnetic nanoparticles not only act as effective tools in water purification, but also help preserve the environment by reducing pollution, using green methods, and being recyclable [18].

Polylactic acid [1] is a renewable, biodegradable biopolymer gaining attention for its role in reducing plastic pollution and environmental harm. Produced from renewable sources like starch and sugars, PLA minimizes reliance on fossil fuels and lowers greenhouse gas emissions. Its biodegradability in soil and water makes it

suitable for applications in packaging, single-use items, and medical fields. However, PLA's degradation rate varies with factors like temperature, humidity, and microbial activity, sometimes persisting like traditional plastics. Advancing technologies to accelerate PLA decomposition and raising awareness about sustainable waste management are crucial to fully harness its ecological benefits[19-21].

As sustainable adsorbents for wastewater treatment, chitosan-based beads have attracted significant attention due to their high efficiency and environmental adaptability. Chitosan, which is obtained from crustacean shells and food waste, is not only a renewable material, but it also helps reduce biowaste. These beads are capable of removing a wide range of contaminants, including heavy metals, paints, and organic matter, from wastewater, and have fewer negative impacts on the environment compared to traditional adsorbents. The biodegradability of chitosan makes it easy to decompose in nature after use, preventing the accumulation of chemical waste. In addition, the process of producing these beads consumes less energy and reduces greenhouse gas emissions. However, challenges such as improving the adsorption capacity and mechanical stability of these beads in various environments remain. The development of new technologies to overcome these limitations and promote the widespread use of these adsorbents can play an important role in improving water quality and protecting the environment[22, 23].

One of the techniques of green synthesis method is the use of plant extracts that by using their existing regenerative compounds, can cause the regeneration of metal salts to metal ions. In recent years, coated magnetic nanoparticles have gained new and diverse applications in both industry and medicine, thanks to their unique properties[24, 25].

Modification of the surface area of these nanoparticles by plant extract increases their efficiency and efficiency in the field of absorption of dangerous dyes and inorganic pollutants. Also, due to their good antibacterial and anti-inflammatory activities, they can be used in the biological field, three main steps in the preparation of nanoparticles that should be evaluated from the point of view of green chemistry, selection of solvent used for synthesis, selection of safe reducing material and selection of non-toxic material for the fixation of nanoparticles. In this work, the extract of *Artemisia absinthium* (Wormwood) plant was used for the synthesis of iron nano particles, and then polylactic acid and nanochitosan and the extract of that plant were used to improve the antioxidant and antibacterial properties of the film.

This work represents a significant advance by demonstrating a fully integrated and green synthesis and application route for active packaging. The method goes beyond simple plant extract synthesis by: Using the extract for the green synthesis of iron nanoparticles, which are then coated with chitosan to improve compatibility and functionality, and successfully embedding these bio-based nanocomposites in a PLA matrix. Comprehensive characterization (physicochemical, mechanical,

antibacterial, antioxidant, and morphological) establishes clear structure-property relationships. Furthermore, formal greenness assessment of the method using AGREEprep software adds a measurable criterion for sustainability and provides a reproducible model for the development of high-performance and environmentally friendly packaging materials.

MATERIAL AND METHOD

Material

Throughout the project, ethanol, $\text{FeCl}_3 \cdot 6\text{H}_2\text{O}$, distilled water, acetic acid, chloroform and chitosan were utilized as materials. $\text{FeCl}_3 \cdot 6\text{H}_2\text{O}$, distilled water, acetic acid, chloroform was purchased in pure form from Merck. PLA (Poly (L-lactic acid), Mw = 80,000, 3 mm particle size) was obtained from Macklin Biochemical Co., Ltd. (China) and dried at 50 °C for 24 hours. Food-grade chitosan with over 95% deacetylation was supplied by Zhuhai Weijia Food Additives Co., Ltd. and plant samples were obtained from fruit sellers located in the northwest region of Iran. Statistical methods were used using AGREE software.

Preparation of Wormwood Ethanolic Extract

Plant collection and extraction.

Dried wormwood aerial parts were pulverized using a laboratory mill and passed through a 40-mesh sieve. The resulting powder was stored in airtight containers at 4°C protected from light.

The ethanolic extract was prepared by maceration. Briefly, 250 g of dried powder was soaked in 400 mL of 96% ethanol (1:1.6 w/v) in a glass flask. The mixture was continuously stirred at 150 rpm using a magnetic stirrer at room temperature ($25 \pm 2^\circ\text{C}$) for 48 h in the dark. The extract was then filtered through Whatman No. 1 filter paper, concentrated under reduced pressure at 40°C using a rotary evaporator, and finally dried in a vacuum oven at 35°C. The dried extract was stored at -20°C until further use.

Green Synthesis of Iron Nanoparticles

Iron oxide nanoparticles were synthesized via a green route using wormwood ethanolic extract as reducing and stabilizing agent. $\text{FeCl}_3 \cdot 6\text{H}_2\text{O}$ (0.135 g) was dissolved in 50 mL double-distilled water to prepare a 0.01 M solution. Wormwood extract (150 mL) was added dropwise to the iron salt solution under vigorous stirring (500 rpm) at room temperature. An immediate color change from pale yellow to dark brown indicated the formation of nanoparticles. Stirring was continued for 1 h, after which the pH was adjusted to 9.0 by dropwise addition of 0.1 M NaOH under continuous monitoring with a calibrated pH meter.

The precipitated nanoparticles were collected by centrifugation at $2000 \times g$ for 10 min, washed three times with double-distilled water and once with absolute ethanol, and dried in a hot air oven at 50°C for 48 h. The dried nanoparticles were stored in a desiccator until further use.[26, 27].

Coating of iron nanoparticles with chitosan

Chitosan-coated magnetic iron oxide nanoparticles were prepared by a modified suspension cross-linking method

[based on Radwan et al.]. Chitosan (25 g) was dissolved in 500 mL of 2% (v/v) aqueous acetic acid to obtain a 5% (w/v) solution. Dried Fe₃O₄ nanoparticles (1 g) were dispersed in this solution by sonication for 30 min.

The dispersion was added dropwise to 140 mL liquid paraffin containing 2.5 mL Span-80 under ultrasonic agitation (200 W) for 30 min at room temperature. Glutaraldehyde (15 mL, 25% aqueous solution) was then added, and cross-linking was allowed to proceed under magnetic stirring (400 rpm) for 5 h. The resulting nanoparticles were magnetically separated, washed sequentially with acetone, ethanol, and distilled water (three times each), and finally dried under vacuum at 80°C for 3 h.

Preparation of Active Polylactic Acid [1] Films

Active PLA films incorporated with chitosan-coated iron oxide nanoparticles and wormwood extract were fabricated by the solvent casting method. PLA [28] was dissolved in 5 mL chloroform under magnetic stirring (600 rpm) for 1 h at room temperature. Separately, chitosan-coated nanoparticles (corresponding to 3% w/w relative to PLA) and wormwood extract (5% w/w relative to PLA) were dispersed in 5 mL chloroform by probe sonication for 1 min.

The nanoparticle/extract dispersion was mixed with the PLA solution and stirred for an additional 30 min. The homogeneous mixture was cast onto glass Petri dishes (9 cm diameter) and allowed to dry at room temperature (25 ± 2°C, 40% relative humidity) for 48 h in a fume hood. The dried films (thickness approximately 80–100 μm) were carefully peeled off and conditioned in a desiccator until analysis.

Sensitivity to the pH of the films

The study examined pH sensitivity—a crucial assessment criterion for smart packaging—and demonstrated how changes in pH can affect the structural response of anthocyanins within the film, leading to observable color changes. Sensitivity to pH and apparent color changes are shown in pH=2 to pH=13 (with phosphate buffer 0.5 M). Hydrochloric acid (HCl) was prepared by distilled water to different pH solutions. The solution containing synthesized nanoparticles and plant extract separately poured into 8 petri dishes and added different buffers with different pH and color change was observed.

Humidity Test

A sample of the film, weighing 50 mg, was subjected to a temperature of 105 °C in an oven for incubation. Subsequently, the film was allowed to cool within a desiccator and its mass was recorded at hourly intervals. This process of measurement persisted until the weight of the film stabilized, with a precision of up to 1 mg. The moisture content present in the film was determined using a specific calculation according to equation 1.

$$\text{Humidity (\%)} = \frac{\mu_i - \mu_f}{\mu_i} \times 100 \quad (1)$$

where μ_i and μ_f are the initial and final weights of the film, respectively.

Solubility Test

Rectangular specimens measuring 5 cm by 5 cm were submerged in a neutral pH buffer solution for a duration of 24 hours. Subsequent to this immersion, the samples were subjected to drying at a temperature of 105 degrees Celsius. The percentage of solubility was then determined using the specified mathematical expression (equation 2).

$$\text{Solubility (\%)} = \frac{\mu_D \times (1 - \mu_c) - \mu_f}{\mu_D \times (1 - \mu_c)} \times 100 \quad (2)$$

where μ_D and μ_f are the original weight and final weights of the film, and μ_c is the moisture content of the film respectively.

Thickness Test

The thickness of the produced films was measured by calipers with an accuracy of 0.04 cm and in 5 points of film samples.

Water vapor permeability (WVP)

To investigate the water vapor permeability (WVP) characteristics, samples of edible films were evaluated using a revised approach derived from the ASTM E96-95 standard. The formula used to calculate the WVP for synthetic polymer films was adapted from the subsequent equation 3:

$$\text{WVP} = (J_{AZ} \cdot \Delta z) / (P_{A1} - P_{A2}) \quad (3)$$

In this context, Δz represents the thickness of the film in millimeters, j_{AZ} denotes the swift movement of water vapor across the film, which is typically influenced by the rate of water vapor transmission. The term $(P_{A1} - P_{A0})$ refers to the differential in partial pressure of water vapor in kilopascals on either side of the film, acting as the impetus for moisture migration. The pressure differential at 100% humidity was established as 3.179 kPa based on the saturated steam table values. The value of j_{AZ} was empirically calculated using the specified equation 4.

$$J_{AZ} = \Delta W / A \Delta t \quad (4)$$

Δt : the time period for moisture transfer

A: the testing surface area of the film sample

In this experiment, laboratory cups with a 12 cm inner diameter holding 4 mL of distilled water were utilized. This volume of water was sufficient to achieve 100% humidity within each cup. The film samples under examination were secured over the openings of these cups, with their perimeters sealed using paraffin wax, ensuring no additional openings for vapor release except through the film itself. Subsequently, these cups were placed in a desiccator filled with calcium chloride to absorb moisture. The entire setup was then incubated at 24 °C for a duration of 24 hours. After this period, the reduction in weight of the cups due to water vapor transmission was measured.

Antibacterial Capacity

The antibacterial effectiveness of film samples was tested using the agar disk diffusion method, focusing on Gram-positive *Staphylococcus aureus* and Gram-negative *E. coli* bacteria. The inhibitory zones were measured accurately in

millimeters. To conduct the test, film samples were cut into 10 mm discs. An 80 μL solution of active bacteria was evenly distributed across LB agar plates. The film discs were then placed onto the inoculated agars, which were incubated at 37°C for 24 hours[29].

Evaluation of DPPH radical trapping ability as an antioxidant index in films

DPPH radicals entrapment activity, films were evaluated. For this purpose, 0.1 g of the film was cut into small pieces and mixed with 2 mL methanol. This mixture was stored for 3 min and then stored at room temperature for 3 hours. After 3 minutes the vortexer and 10 min centrifugation (2300 rpm) were used to evaluate the activity of DPPH radical trapping.

The resulting mixture was stored for 1 minute and then 30 min at room temperature and in a dark place. Methanol was used as a control. For this purpose, 2 ml of methanol solution DPPH 0.06 mM was added to 500 μL methanol and its absorption was read at 517 nm[30].

Characterization

At this point in the research, the properties of the developed films were evaluated through various analytical techniques including Fourier Transform Infrared Spectroscopy (FTIR), Scanning Electron Microscopy (SEM), and X-Ray Diffraction (XRD) to examine the characteristics of both the films and the nanoparticles.

The SEM analysis involved cutting grape extract film samples into roughly 1 cm by 1 cm pieces. These samples were then coated with gold by the SEM technician to boost electrical conductivity, improving their interaction with electrons. Finally, the samples were placed in a specific chamber within the equipment and imaged at different magnifications.

In the FTIR spectroscopy process, the film specimens were encapsulated between two clear layers of potassium bromide and positioned within a dedicated chamber to capture the absorption spectra. The creation of alumina nanoparticles utilized the potassium bromide pellet method, taking advantage of the material's transparency to infrared radiation. During the pellet preparation, alumina was meticulously pulverized together with potassium bromide in a mortar with a pestle until achieving a particle size smaller than 2 μm . Subsequently, this mixture was compressed into a slender pellet and subjected to analysis over a wavenumber spectrum ranging from 400 to 4000 cm^{-1} .

In preparing samples for X-ray diffraction (XRD), a small quantity, generally several tenths of a gram, of the substance is finely pulverized using a mortar. This process reduces surface energy and helps avoid shifts in the diffraction peaks. It is preferable for the powder particles to be smaller than 10 micrometers in size. Once prepared, the sample is evenly distributed across a sample holder and subjected to X-ray exposure[31].

Assessment of Greeness

The AGREEprep software was used to assess the environmental compatibility of the method. This involved assessing various parameters related to toxic substances,

waste and resource use based on specific criteria and penalties. Scores are assigned across ten different assessment parameters. And it assigns scores between 0 and 1, where these boundaries indicate the weakest and most outstanding performance, respectively. Each criterion has a predetermined weight that contributes to the overall score, although evaluators are allowed to adjust these weights based on their analytical needs, provided that they justify their decisions. The scores of the criteria are adjusted based on the weights and summed into a final score, also ranging from 0 to 1, with the highest value indicating the best possible performance. The AGREEprep software collects input from all ten steps and, upon completion of the assessment, creates a circular pictogram with a central area representing the overall score surrounded by ten trapezoidal bars – one for each criterion – of varying length. After assessment, the software changes the color of each element based on the assigned weight equivalent, providing a clear visual representation of the strengths, weaknesses and individual contributions of the method to the overall score. Green areas indicate the environmental safety and compatibility of each part of the method, while red indicates high risk, highlighting concerns during preparation, production and use[32].

RESULTS

The reason for using wormwood extract in this work is the antimicrobial and antioxidant properties of this plant. The higher the concentration of wormwood extract, the more effective these properties will be and the food coating will be. However, the physical properties of the films should also be taken into account. At low concentrations of the extract in the produced film, the effect on the stability and permeability is low, and at medium concentrations it will improve the physical properties, but at high concentrations it will reduce flexibility and increase stiffness. In the case of the latter film, as written in the antioxidant chart, a concentration of 1 to 7% of the extract was used, but at concentrations of 5%, the most desirable state of the film was seen in terms of appearance, ease of separation from the substrate and flexibility. Therefore, choosing the right concentration is important to achieve the best results in maintaining the quality and safety of food and the usability of the film. The appearance of the synthesized film of polylactic acid and iron nanowires and chitosan with *Artemisia absinthium* (Wormwood) extract is presented in Figure 1. After optimizing the effective parameters in membrane manufacturing, it can be introduced as a suitable and efficient food coating.

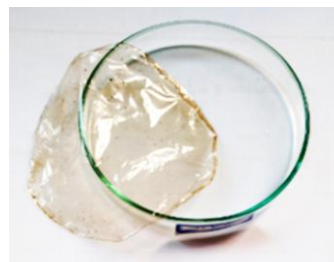


Fig. 1. The appearance of the synthesized film of polylactic acid and iron nanowires and chitosan with *Artemisia absinthium* (Wormwood) extract

Characterization of prepared nanoparticles and film

For careful study, the structure and morphology of them with identification and measurement devices is required, depending on the type and material produced, the relevant analyzer is selected. In this work, various devices such as SEM, FTIR, XRD were used to evaluate each case.

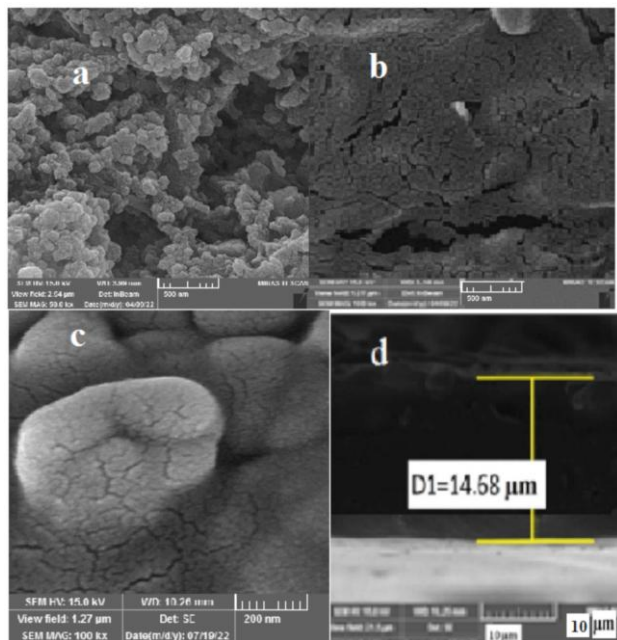


Fig. 2. a: SEM image of a:iron nanoparticles made by green synthesis, b: nanoparticles coated with chitosan, c: the surface and d: the cross section of film.

The results of green synthesis of iron nanoparticles and its confirmation tests, reaction of reduction of iron salt solution at room temperature after adding dried extract to the iron salt solution was done and color change was obtained, indicating that iron nanoparticles were produced. After centrifuging for 10 minutes with 2000 rpm iron nanoparticles sedimentation, the resulting dark colored solution was washed for several steps and its dried powder was used for SEM analysis. Scanning electron microscopy obtained from magnetic iron nanoparticles under optimal conditions shows the synthesis of spherical nanomaterials (Figure.2a).

Electron microscope images obtained from iron nanoparticles coated with chitosan are presented (Figure.2b). Also, in Figure 2c and d, the surface and cross-section of the film that was broken with liquid nitrogen are shown respectively. The pores observed in the structure of all the produced films were due to high volatility of chloroform and its evaporation during drying,

According to the presented figure, the XRD spectrum of the packaging film containing PLA, iron nanoparticles, chitosan and wormwood extract shows a mixture of crystalline and amorphous phases. Characteristic peaks related to PLA are observed at angles of 16.7° (110), 19.1° (203), and 22.4° (015), confirming the semi-crystalline structure of this polymer. The decrease in the intensity of these peaks can be due to interactions between PLA and

other components such as iron nanoparticles, chitosan and wormwood extract. Iron nanoparticles, which usually appear as iron oxide (Fe_2O_3 or Fe_3O_4), give rise to characteristic peaks at angles of 30.1° (220), 35.5° (311), 43.1° (400), and 57.1° (511). The presence of these peaks indicates a uniform distribution and lack of particle aggregation in the film structure. Chitosan, due to its amorphous structure, produces a broader peak in the range of $20\text{-}25^\circ$. Wormwood extract may also produce weak peaks in the range of $10\text{-}30^\circ$, but usually due to the low concentration, their effect is dominated by other peaks. Interactions between different film components, such as the formation of hydrogen bonds between the carbonyl groups of PLA and the hydroxyl groups of chitosan or extract, can lead to changes in their crystalline and amorphous structure. These changes indicate that the addition of nanoparticles and extract not only affects the film structure, but can also improve its mechanical and functional properties. Finally, these analyses confirm that the fabricated packaging film has a stable and consistent structure that can be used as a sustainable and efficient alternative in the food industry. (Figure.3).

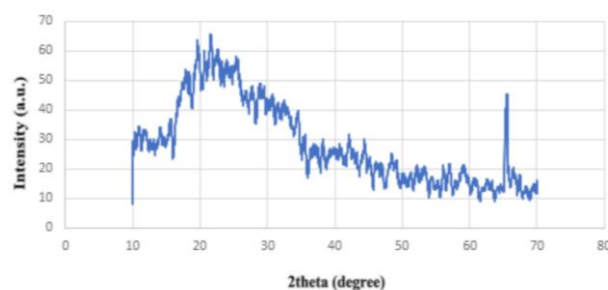


Fig. 3. XRD of the synthesized film.

Infrared absorption spectra of magnetic nanoparticles, containing methanol extract of wormwood indicate the presence of OH functional groups as well as C-H is aliphatic and aromatic, as well as the carbonyl group, which is similar to the secondary compounds found in wormwood extract. The spectrum showed strong absorption bands in 1053 cm^{-1} , 1096 , 1261 , 1633 , 2957 , 3417 cm^{-1} . These bands conform to the vibrations of methylene tensile, carbonyl group, aromatic tension, C-H and C-O stretching, FTIR spectra confirms the role of these functional groups in synthesis and stability of magnetic iron nanoparticles by biotransformation of wormwood extract(Figure4.a).

The lower figure of FTIR spectra shows chitosan. In the chitosan spectrum, the peaks in the range $3200\text{-}3400\text{ cm}^{-1}$ are a combination of the O-H tensile groups and the hydrogen intramolecular bond, the peak of 1654 cm^{-1} in Chitosan corresponds to R-CO-NH₂ groups in the chitosan nanoparticle spectrum. The spectrum in regions between $1000\text{-}1250\text{ cm}^{-1}$ is related to TPP, and the two peaks in 1576 and 1411 cm^{-1} of the flexion group indicate the formation of interacting and this peak NH₄ is between the two peaks in the 1576 and 1411 cm^{-1} of the flexion group. The phosphate groups are TPP and the amino groups are chitosan (Figure4.b).

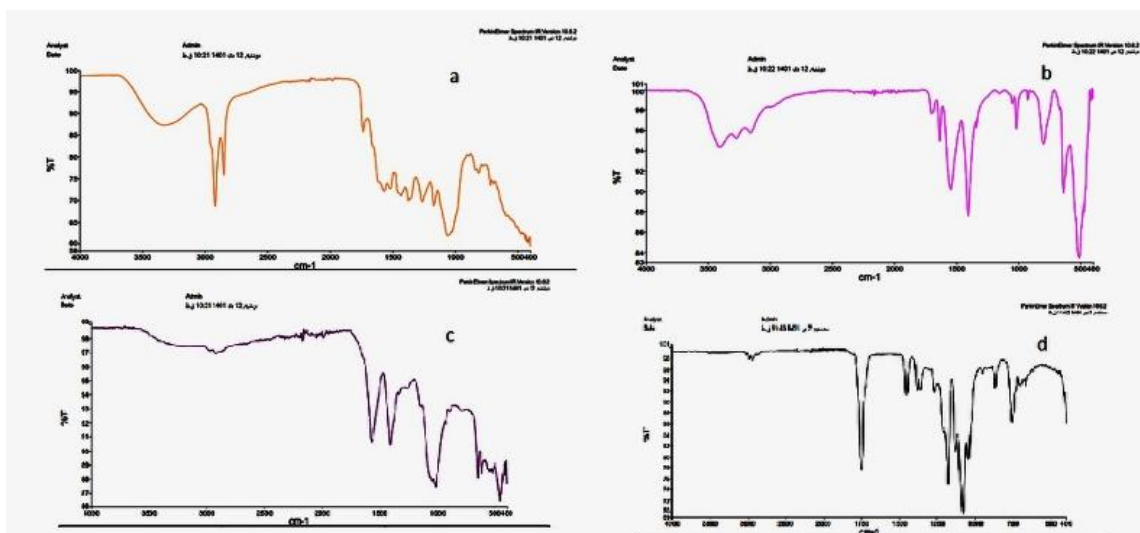


Fig. 4. FTIR spectra of wormwood extract.(a), chitosan(b), chitosan-coated magnetic nanoparticles(c), and of the synthesized film(d)

The FT-IR spectra of chitosan-coated magnetic nanoparticles is shown in the figure that the vibrational spectrum of N-H amine and hydroxyl functional groups in 13450 cm^{-1} , the vibration-tensile spectra of C=O amides in 1663 cm^{-1} , the flexural vibration spectrum of the amine groups at 1603 cm^{-1} and the tensile vibrations of the C-OH groups in 1082 cm^{-1} were observed. Most studies have shown that amines and hydroxyl groups react with Fe^{+3} in magnetic chitosan. Therefore, the peaks observed in chitosan are moved to 1590 , 1634 and 3418 cm^{-1} , respectively, and a new peak of Fe-O vibrations in Fe_3O_4 appears in the 573 cm^{-1} region (Figure 4.c). And finally, the spectrum of the synthesized film (Fig4.d). The peak at position 858 cm^{-1} is related to the C-H group of lactic acid polymer and the peak at position 1031 cm^{-1} is related to C-OH deformation, while the peak at position 1057 cm^{-1} is related to the C-O elasticity of carbon 6. The observed peaks in the range of 1120 and 1250 cm^{-1} are related to the symmetric vibration of C-O-C and 1133 respectively. The observed peaks in the range of 1120 and 1250 cm^{-1} are related to the symmetric and asymmetric vibration of C-O-C and the peak of 1333 cm^{-1} indicate the tensile vibration of the C-O-C bonds. The observed peaks at the positions of 1361 - 1365 cm^{-1} and 1381 cm^{-1} respectively are related to symmetric flexural oscillations and symmetric deformation of CH_3 groups while the peak at the positions of 1450 - 1452 and 1433 cm^{-1} represent asymmetric flexural oscillations of CH_3 groups and the peaks in 1746 - 1761 cm^{-1} represent the symmetric elasticity of C=O groups in the esterification bonds and carbonyl lactide groups.

The 2754 and 2766 cm^{-1} peaks correspond to the symmetric and asymmetric vibration of C-H in CH_3 groups, respectively. Peaks in the range 2940 - 3000 cm^{-1} are related to the tensile of CH_3 groups so that the observed peaks in 2946 and 2995 cm^{-1} are related to symmetric and asymmetric vibration of CH_3 groups, respectively. The peak observed in the range of 3100 - 3600 cm^{-1} and especially the position of 3200 cm^{-1} indicates the bonded elasticity of OH groups. O is related.

Study of the physical properties of the prepared film

Average Film Thickness

The film thickness was assessed at five random points on its surface. The average thickness recorded for the film with three replicates for the data was $0.089 \pm 0.01\text{ cm}$.

Humidity (%)

Moisture within layers promotes molecular diffusion and enhances solubility. Therefore, it is crucial to reduce moisture levels when utilizing films for food packaging. As the amount of reinforcement in the polymer matrix increases, both the humidity (%) and water solubility noticeably decrease. The addition of filler nanoparticles also results in diminished humidity (%) and solubility. This effect is likely due to the formation of hydrogen bonds between the hydroxyl groups on the nanoparticle surfaces and the polar groups in the polymer matrix, which strengthens their interactions. Such interactions reduce the availability of hydroxyl groups, thereby enhancing the water resistance of the films. To assess the film's humidity (%), it is necessary to measure the initial and final weights of the films after they have been stabilized at $105\text{ }^\circ\text{C}$. For the film with nanoparticles, the moisture content decreased to $65.61 \pm 3.84\%$, which was a significant reduction compared to the films without nanoparticles. This data was obtained based on three repetitions of the test procedure.

Solubility Assessment

The solubility of the film was assessed using a method comparable to that used for the standard final films and the percentage solubility was calculated. The test was repeated three times and the modified film showed a solubility of $18.09 \pm 2.51\%$, which was consistent with the expected results obtained from the moisture assessments.

Duration of manifestation of sensitivity to the environment

The rapidity with which sensors react to environmental alterations is crucial in their development. This is because

a quicker color transition in a sensor allows for more immediate detection of potential food spoilage, thereby preventing the consumption of compromised products. To evaluate this, the film was submerged in solutions of varying pH levels, and the time until noticeable changes occurred was meticulously recorded. The findings from various conditions indicated that, on average, the sensitivity duration of the film across different pH levels was approximately one minute (Figure.5).

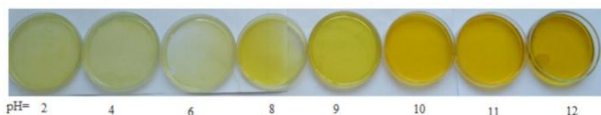


Fig. 5. Investigating the effect of pH on the color change of manufactured films: Analysis and comparison of colors in different acidic and basic conditions

Water vapor permeability test

Water vapor permeability (WVP) is often analyzed in edible films due to its role in processes that contribute to food degradation. Table 1 shows the changes in WVP values for chitosan films injected with iron nanoparticles and wormwood extract. The data show that the incorporation of nanoparticles into the layers reduces their WVP. Furthermore, increasing the concentration of the plant extract is associated with a further reduction in WVP. Wormwood extract: It can reduce water vapor permeability by creating a protective layer. Iron nanoparticles can also help reduce WVP by increasing the density and reinforcing the structure of polymers. Another point in this membrane is the synergy between the two materials. The combination of these two materials can have synergistic effects. So that the properties of both materials together lead to a further improvement in WVP. Wormwood extract may help in better distribution of iron nanoparticles in the polymer matrix and better performance. Chemical bonds The combination of wormwood extract and iron nanoparticles can lead to the creation of new chemical bonds that strengthen the structure and reduce empty space. Also, changes in surface properties: This combination can change surface properties and reduce water vapor permeability. Table 1 shows the effect of the extract and nanoparticles on water vapor permeability. Data were obtained with three replicates.

Table 1

Water Vapor Permeability (WVP) test of the films. Data were obtained with three replicates.

Sample	WVP (mg. mm/m ² .kPa.h)
PLA+C	1.150±0.2
PLA+EX Artemisia absinthium 1%	1.172±0.3
PLA+EX Artemisia absinthium 3%	1.167±0.1

PLA+EX Artemisia absinthium 5%	1.151±0.2
PLA+EX Artemisia absinthium 7%	1.148±0.1
PLA+N _{Fe}	0.829±0.1
PLA N _{Fe} +EX Artemisia absinthium 1%	1.027±0.1
PLA N _{Fe} +EX Artemisia absinthium 3%	1.015±0.1
PLA N _{Fe} +EX Artemisia absinthium 5%	1.008±0.2
PLA N _{Fe} +EX Artemisia absinthium 7%	0.974±0.1

Evaluation of Antioxidant Capacity Using the DPPH Radical Method

The antioxidant activity of various substances is assessed using the DPPH radical method, which is a well-known approach for evaluating the antioxidant capacity of various substances. This technique relies on the neutralization of DPPH radicals by antioxidants in a free radical-free environment. Typically, the effectiveness of a substance is measured against a standard antioxidant such as vitamin C. The DPPH method is of considerable value in sectors such as food, healthcare, and biotechnology, and plays an important role in the discovery and introduction of new antioxidant agents. In this method, the interaction between antioxidants and DPPH radicals leads to a color change in the test medium, which can be quantitatively analyzed using a spectrometer. DPPH itself is characterized by its stability and the presence of an unpaired electron on one of its nitrogen atoms. The basic principle of antioxidant testing is the scavenging of this DPPH radical [33, 34]. DPPH is notable for its purple methanol solution that strongly absorbs light between wavelengths of 519-595 nm. During the test, antioxidants donate an electron to the DPPH radical, which results in a change from purple to yellow color as the absorption at 595 nm decreases. This change in color intensity is measured spectroscopically to determine the antioxidant properties of the material under study. Wormwood extract plays a key role in enhancing the antioxidant properties of this film, so different percentages of this extract were tested in the structure of this film, which can be seen in Figure 6. As can be seen in the figure, the higher the amount of plant extract, the higher the antioxidant properties. In making this film, adding more than 5% wormwood extract would have caused an improper shape in the film when it was separated from the substrate, and it was necessary to add only up to 5% of the extract.

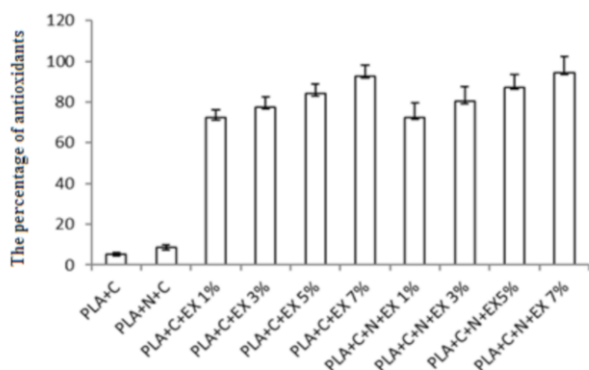


Fig. 6. DPPH radical scavenging activities of films containing poly(lactic acid)[1], nanoparticles(N), chitosan©, and extract extracted from wormwood plant(EX).

Wormwood extract, containing active compounds like polyphenols (e.g., quercetin and rutin), terpenoids (e.g., absinthene), and sesquiterpenes, holds a crucial role in antioxidant activity. Its mode of action involves neutralizing free radicals (such as DPPH and OH^-) through hydrogen donation, suppressing lipid peroxidation in cell membranes, and boosting endogenous antioxidant enzymes like catalase and superoxide dismutase [35]. Nanochitosan, another vital element, contributes to antioxidant activity in two primary ways: firstly, its positive surface charge and functional groups, such as amino and hydroxyl groups, facilitate the absorption of free radicals; secondly, it can chelate metal ions (e.g., Fe^{2+}) that trigger oxidative reactions. Furthermore, nanochitosan bolsters the extract's stability and enhances its sustained release by forming bonds with the wormwood-derived polyphenols, creating a synergetic effect. While iron nanoparticles at high concentrations have the potential to induce oxidative stress by generating reactive oxygen species (ROS), at well-regulated levels and in the presence of other film components, their impact can be positive. They particularly inhibit the Fenton reaction, which generates hydroxyl radicals, by chelating metal ions. In this structure, PLA and nanochitosan mitigate any adverse effects of iron nanoparticles by encapsulating them. Together, these four components exhibit heightened antioxidant capacity, especially driven by the synergy between wormwood extract and nanochitosan. Nanochitosan enhances extract stability, controls its release, and facilitates access to active functional groups through the formation of hydrogen and electrostatic bonds with polyphenols. This collaboration is clearly evident in standard antioxidant tests such as DPPH, where the multi-component film demonstrates superior radical scavenging potential compared to individual films made with separate ingredients. These films have practical applications in active food packaging, where their controlled release of antioxidants limits the oxidation of fats and proteins in food products, extending the product shelf life.

Exploring the Antimicrobial Capabilities of the Developed Films

The film's antibacterial effects against gram-negative bacteria (*E. coli*) and gram-positive bacteria (*S. aureus*) were evaluated with the Disk-Diffusion Method (DDM). The extract from *Artemisia absinthium* demonstrated notable antibacterial effects on both types of bacteria. The inhibition zone's diameter in samples with grape extract was significant, highlighting the strong antimicrobial attributes and effectiveness of Shahani grape extract. This could be attributed to the high concentration of polyphenols, including anthocyanins, present in the grape extract. When incorporated into diffusion disks, this extract exhibited a pronounced inhibitory impact on both gram-negative and gram-positive bacteria. The study revealed that the extract was more potent against gram-positive than gram-negative bacteria. Laboratory findings also indicated that active chitosan packaging and films could be developed using black grape extract, enhancing both antioxidant properties and total phenolic content. The antibacterial activity observed with *Artemisia absinthium* extract suggests its potential use in film structures for the food industry, potentially extending food shelf life (Table 2). Iron oxide nanoparticles have garnered significant attention for their extensive applications across various biomedical domains, particularly in imaging and diagnostics. They are employed in techniques such as magnetic resonance imaging, computed tomography, positron emission tomography, and magnetic hyperthermia for cancer therapy.

Table 2
Examination of antibacterial properties By diameter of containment area (mm).

Sample	<i>S.aureus</i> (+)	<i>E.coli</i> (-)
PLA+EX <i>Artemisia absinthium</i> 1%	30.07±0.1	16.3±0.4
PLA+EX <i>Artemisia absinthium</i> 3%	30.11±0.5	16.37±0.5
PLA+EX <i>Artemisia absinthium</i> 5%	30.18±0.8	16.65±0.6
PLA+EX <i>Artemisia absinthium</i> 7%	30.25±1.2	16.92±0.5

Additionally, Iron oxide nanoparticles are used in cell or molecule separation and biosensor development, with applications spanning immunoassays, neuroelectronic research, and biomedical imaging. They also show potential for imaging and monitoring brain cells in vivo. Furthermore, Iron oxide nanoparticles have demonstrated their capability to deliver drugs and viral vectors to specific target cells effectively. Of special interest is their notable antibacterial activity, offering promise in addressing the global challenge of antibiotic-resistant bacterial strains. For instance, their direct bactericidal effects have been exemplified with *S. aureus*. Beyond their antimicrobial properties, Fe_3O_4 nanoparticles contribute to advancements in regenerative medicine. Importantly, Iron oxide nanoparticles exhibit excellent biocompatibility in

both in vivo and in vitro environments, setting them apart from ZnONPs, which exhibit elevated cytotoxicity. This balanced combination of antibacterial efficiency and biocompatibility establishes Iron oxide nanoparticles as an attractive candidate for the development of next-generation antimicrobial agents[36].

Assessment of the method's greenness

Using the AGREEprep software, the method achieved a greenness score of 0.80, as indicated in the pictogram. The circular diagram revealed that the parameter scores are nearly in the green range. Consequently, based on the predominant color in the icon and the numerical outcome, there is reason to be optimistic about the method's environmental compatibility and overall greenness (Figure7).

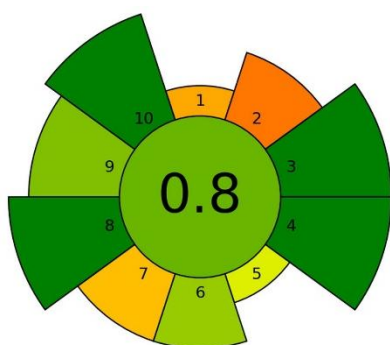


Fig. 7. Assessment of the method's greenness

Practical Applications and Potential Industrial Relevance

The multifunctional PLA-based nanocomposite film developed in this study holds significant practical potential for real-world applications in the food packaging industry. Its strong antimicrobial properties, with large inhibition zones against both Gram-positive (*S. aureus*) and Gram-negative (*E. coli*) bacteria, make it particularly suitable for active packaging of highly perishable foods prone to microbial contamination, such as fresh red meat, poultry, fish, seafood, and dairy products (e.g., cheese). By inhibiting bacterial growth through the synergistic action of wormwood polyphenols and chitosan-coated iron oxide nanoparticles, the film can substantially extend shelf life, reduce food spoilage, and enhance food safety during storage and transportation.

The high antioxidant activity, driven primarily by the polyphenolic compounds in wormwood extract (e.g., quercetin and rutin), offers effective protection against lipid oxidation and rancidity. This feature is especially valuable for packaging oxidation-sensitive products, including oily fish, nuts, fried snacks, and fresh-cut fruits and vegetables, where it can delay discoloration, off-flavor development, and nutrient loss, thereby maintaining sensory and nutritional quality over an extended period.

A key intelligent functionality of the film is its visible pH-responsive color change across a broad range (pH 2–13), which enables on-package, real-time monitoring of food freshness without destructive testing. This property is highly relevant for protein-rich foods that release volatile amines during spoilage (e.g., meat, fish, and shrimp), causing pH increases that trigger noticeable color shifts. Such visual indicators empower both retailers and consumers to assess product quality at a glance, reducing food waste due to premature discarding of safe products or consumption of spoiled ones.

From an environmental and industrial perspective, the film's fully biodegradable PLA matrix, combined with its green synthesis route (AGREEprep score of 0.80), positions it as a sustainable alternative to conventional petroleum-based plastics like polyethylene and polypropylene. The solvent-casting fabrication method is simple, scalable, and compatible with existing industrial film production lines, facilitating potential commercialization. Overall, this nanocomposite film addresses current demands for eco-friendly, active, and intelligent packaging solutions that simultaneously improve food safety, extend shelf life, minimize waste, and support circular economy goals in the global food supply chain. Future studies could focus on pilot-scale production and real-food storage trials to further validate its performance under commercial conditions.

DISCUSSION

The comparative analysis presented in Table 3 underscores the advancements in our PLA-based nanocomposite film incorporating chitosan-coated iron oxide nanoparticles and wormwood (*Artemisia absinthium*) extract, positioning it as a promising material for active and intelligent food packaging. When benchmarked against similar studies, our film demonstrates competitive or superior performance across multiple key properties, highlighting the synergistic effects of its components.

Table 3
Comprehensive Comparison of Key Properties in PLA/Chitosan-Based Nanocomposite Films for Food Packaging Applications.

Study (Year)	Film Composition	Antimicrobial Activity (Inhibition Zone, mm)	Mechanical Properties (Tensile Strength / Elongation at Break)	pH Sensitivity (Color Change)	Other Properties (e.g., WVP Reduction, Antioxidant)	Comparison with Present Study
Present Study	PLA + Chitosan-coated Fe ₃ O ₄ + Wormwood extract (3–5%)	<i>S. aureus</i> : 30.25 ± 1.2 <i>E. coli</i> : 16.92 ± 0.53	Flexibility improved at 5% extract; balanced stiffness	Visible color change (pH 2–13)	Reduced WVP (synergistic); High DPPH scavenging at 5% extract	-

Noshirvani et al. (2017) [1]	PLA + Chitosan + Essential oils (clove/argan)	Strong against <i>E. coli</i> / <i>S. aureus</i> (higher with rough coating)	Improved ductility/flexibility without plasticizer	Not reported	High antioxidant; Good barrier	Similar antimicrobial/antioxidant synergy, but present study superior inhibition zones due to wormwood + Fe ₃ O ₄
Qin et al. (2019) [2]	Chitosan + AgNPs + Purple corn extract	Enhanced against Gram+/- bacteria	Improved tensile strength/barrier	pH-sensitive (anthocyanin-based)	Strong antioxidant	Comparable pH sensitivity and antimicrobial, but present study uses green Fe ₃ O ₄ (safer than AgNPs)
Alizadeh-Sani et al. (2021) [3]	Chitosan + Metal oxides (ZnO/TiO ₂)	15–19 mm against foodborne pathogens	Enhanced tensile/modulus	Not primary focus	Reduced WVP; UV barrier	Similar mechanical/WVP improvements; present study better Gram+ inhibition via wormwood synergy
Coneo et al. (2023) [4]	Chitosan/PVA + ZnO NPs	Strong against <i>S. aureus</i> / <i>E. coli</i>	Increased tensile strength	Not reported	Improved barrier/antibacterial	Comparable antimicrobial, but present study incorporates PLA for biodegradability + pH intelligence
Mohamed et al. (2024) [5]	Shellac/Chitosan + Spinel NPs (ZnAl ₂ O ₄ /CuAl ₂ O ₄)	Broad-spectrum antibacterial	Good tensile/elongation	Not reported	High air permeability control	Similar mechanical enhancements; present study unique with wormwood for antioxidant + pH response

[1] Noshirvani et al., *Materials* (2017). [2] Qin et al., *Food Hydrocolloids* (2019). [3] Alizadeh-Sani et al., *PMC* (2021). [4] Coneo et al., *Polymer Bulletin* (2023). [5] Mohamed et al., *Scientific Reports* (2024).

This table demonstrates that the present PLA-based film exhibits superior synergistic performance, particularly in antimicrobial activity against Gram-positive bacteria, pH-responsive color change (ideal for intelligent packaging), and balanced mechanical properties with natural wormwood extract, outperforming or matching similar nanocomposites while maintaining green synthesis principles.

In terms of antimicrobial activity, our film exhibits notably larger inhibition zones against both Gram-positive (*S. aureus*: 30.25 ± 1.2 mm) and Gram-negative (*E. coli*: 16.92 ± 0.53 mm) bacteria compared to most referenced works. For instance, Noshirvani et al. (2017) reported strong inhibition with PLA-chitosan films enhanced by essential oils, but our formulation achieves greater efficacy, likely due to the combined action of wormwood's polyphenolic compounds (e.g., quercetin and rutin), which disrupt bacterial cell membranes, and the reactive oxygen species (ROS) generated by iron oxide nanoparticles. This synergy outperforms the metal oxide-based films in Alizadeh-Sani et al. (2021), where zones ranged from 15–19 mm, and even surpasses the ZnO nanoparticle systems in Coneo et al. (2023), suggesting that our green-synthesized Fe₃O₄ nanoparticles provide a safer, more potent alternative without the cytotoxicity concerns associated with silver or zinc oxides.

Regarding mechanical properties, our film strikes a balance between flexibility and stiffness at 5% wormwood extract concentration, which is comparable to the

enhanced tensile strength and ductility observed in Qin et al. (2019) and Mohamed et al. (2024). The incorporation of chitosan as a coating not only improves interfacial adhesion within the PLA matrix but also mitigates brittleness often seen in pure nanoparticle composites, as evidenced by the improved elongation at break in similar spinel nanoparticle films. This mechanical resilience is crucial for practical food packaging applications, ensuring the film withstands handling and storage without compromising integrity.

The pH sensitivity of our film, manifesting as visible color changes across a broad pH range (2–13), aligns well with anthocyanin-based systems in Qin et al. (2019), where purple corn extract enabled similar responsive behavior. However, our use of wormwood extract introduces a novel, naturally derived indicator that is less explored in literature, offering a cost-effective and eco-friendly option for monitoring food spoilage through volatile amine detection or pH shifts in perishable goods. This feature sets our work apart from studies like Coneo et al. (2023) and Alizadeh-Sani et al. (2021), which focused

more on barrier properties without emphasizing intelligent functionality.

Additionally, our film's reductions in water vapor permeability (WVP) and high DPPH radical scavenging activity at optimal extract levels mirror the barrier enhancements in Noshirvani et al. (2017) and Alizadeh-Sani et al. (2021), but with added antioxidant benefits from wormwood's terpenoids and sesquiterpenes. The hydrogen bonding between chitosan's hydroxyl/amino groups and PLA's carbonyls, combined with the nanofiller effect of Fe₃O₄, likely contributes to a denser matrix that minimizes moisture ingress and oxidative degradation, extending shelf life more effectively than the PVA-chitosan blends in Coneo et al. (2023).

Overall, these comparisons reveal that our nanocomposite film not only matches but often exceeds the performance of prior formulations in multifunctional aspects, owing to the eco-friendly green synthesis and targeted integration of bioactive components. This approach addresses key challenges in sustainable packaging, such as reducing plastic waste and enhancing food safety, and paves the way for further optimization in industrial applications.

CONCLUSIONS

In this study, a novel biodegradable active and intelligent food packaging film was successfully developed based on polylactic acid [1] incorporated with chitosan-coated iron oxide nanoparticles green-synthesized using *Artemisia absinthium* (wormwood) extract. The key findings demonstrate that this nanocomposite offers multifunctional performance superior to many reported systems.

The film exhibited outstanding antimicrobial activity, with inhibition zones reaching 30.25 ± 1.2 mm against *Staphylococcus aureus* and 16.92 ± 0.53 mm against *Escherichia coli* – significantly larger than those observed in comparable chitosan-metal oxide or plant extract-based films. This enhanced efficacy is attributed to the strong synergistic interaction between the polyphenolic compounds in wormwood extract, the functional groups of nanochitosan, and the controlled ROS generation from iron oxide nanoparticles.

Excellent antioxidant capacity was achieved, with DPPH radical scavenging activity increasing markedly with wormwood extract concentration up to the optimal 5% level, beyond which film appearance and flexibility were compromised. This balance ensured both high bioactive performance and practical usability.

The film displayed clear pH-responsive color changes across a wide range (pH 2–13), enabling its potential use as an intelligent indicator for real-time monitoring of food spoilage. Physical properties were also improved: water vapor permeability was substantially reduced due to synergistic barrier effects of the nanoparticles and extract, while moisture content ($65.61 \pm 3.84\%$) and solubility ($18.09 \pm 2.51\%$) confirmed good stability. Structural analyses (SEM, FTIR, XRD) verified uniform nanoparticle distribution and successful integration within the PLA matrix.

Importantly, the entire synthesis process achieved a high greenness score of 0.80 according to AGREEprep evaluation, underscoring its environmental compatibility.

Overall, this work introduces a sustainable, efficient, and multifunctional PLA-based nanocomposite film that combines potent antimicrobial and antioxidant properties with intelligent pH-sensing capability. By utilizing green-synthesized nanoparticles and a natural plant extract at optimized concentrations, the developed film represents a promising alternative to conventional petroleum-based packaging, contributing significantly to extended food shelf life, reduced food waste, and environmental sustainability in the food industry.

Conflict of interest

The authors have no conflicts of interest.

References

- [1] Plamadiala I, Croitoru C, Pop MA, Roata IC. Enhancing polylactic acid (PLA) performance: A review of additives in fused deposition modelling (FDM) filaments. *Polymers*. 2025;17(2):191.
- [2] Etemadi H, Afsharkia S, Zinatloo-Ajabshir S, Shokri E. Effect of alumina nanoparticles on the antifouling properties of polycarbonate-polyurethane blend ultrafiltration membrane for water treatment. *Polymer Engineering & Science*. 2021;61(9):2364-75.
- [3] Zinatloo-Ajabshir S, Morassaei MS, Salavati-Niasari M. Eco-friendly synthesis of Nd₂Sn₂O₇-based nanostructure materials using grape juice as green fuel as photocatalyst for the degradation of erythrosine. *Composites Part B: Engineering*. 2019;167:643-53.
- [4] Zinatloo-Ajabshir S, Salavati-Niasari M. Preparation of magnetically retrievable CoFe₂O₄@ SiO₂@ Dy₂Ce₂O₇ nanocomposites as novel photocatalyst for highly efficient degradation of organic contaminants. *Composites Part B: Engineering*. 2019;174:106930.
- [5] Zinatloo-Ajabshir S, Yousefi A, Jekle M, Sharifianjazi F. *Carbohydrate Polymer Technologies and Applications*.
- [6] Rezayeenik M, Mousavi KM, Zinatloo AS. Development of CeVO₄/rGO nanocomposite via sonochemical synthesis for high-capacity electrochemical hydrogen storage. 2025.
- [7] Roy S, Ghosh T, Zhang W, Rhim J-W. Recent progress in PBAT-based films and food packaging applications: A mini-review. *Food Chemistry*. 2024;437:137822.
- [8] Roy S, Priyadarshi R, Ezati P, Rhim J-W. Curcumin and its uses in active and smart food packaging applications-A comprehensive review. *Food Chemistry*. 2022;375:131885.
- [9] Singaram AJV, Guruchandran S, Ganesan ND. Review on functionalized pectin films for active food packaging. *Packaging Technology and Science*. 2024;37(4):237-62.
- [10] Palaniyappan S, Sivakumar NK, Bodaghi M, Rahaman M, Pandiaraj S. Preparation and

- performance evaluation of 3D printed Poly Lactic Acid composites reinforced with silane functionalized walnut shell for food packaging applications. *Food Packaging and Shelf Life*. 2024;41:101226.
- [11] Barmdaki AA, Paul UC, Nardi M, Athanassiou A. Eco-friendly Blends of Polylactic Acid and Polyhydroxybutyrate Enhanced with Epoxidized Soybean Oil Methyl Ester for Food-Packaging Applications. *ACS Applied Polymer Materials*. 2024.
- [12] Lawal U, Kumar N, Samyuktha R, Gopi A, Robert V, Pugazhenth G, et al. Poly (lactic acid)/amine grafted mesoporous silica-based composite for food packaging application. *International Journal of Biological Macromolecules*. 2024:134567.
- [13] da Silva Pens CJ, Klug TV, Stoll L, Izidoro F, Flores SH, de Oliveira Rios A. Poly (lactic acid) and its improved properties by some modifications for food packaging applications: A review. *Food Packaging and Shelf Life*. 2024;41:101230.
- [14] Kumari SVG, Pakshirajan K, Pugazhenth G. Recent advances and future prospects of cellulose, starch, chitosan, polylactic acid and polyhydroxyalkanoates for sustainable food packaging applications. *International Journal of Biological Macromolecules*. 2022;221:163-82.
- [15] Stoleru E, Vasile C, Irimia A, Brebu M. Towards a bioactive food packaging: Poly (lactic acid) surface functionalized by chitosan coating embedding clove and argan oils. *Molecules*. 2021;26(15):4500.
- [16] Deng J, Yu W, Zhan L, Zhu X, Fang Y, Zhang P, et al. Wettability Regulation of Membranes Based on Biodegradable Aliphatic Polyester. *Journal of Membrane Science*. 2024:123199.
- [17] Ijaz I, Gilani E, Nazir A, Bukhari A. Detail review on chemical, physical and green synthesis, classification, characterizations and applications of nanoparticles. *Green chemistry letters and reviews*. 2020;13(3):223-45.
- [18] Abdel Maksoud M, Fahim RA, Bedir AG, Osman AI, Abouelela MM, El-Sayyad GS, et al. Engineered magnetic oxides nanoparticles as efficient sorbents for wastewater remediation: a review. *Environmental Chemistry Letters*. 2022;20(1):519-62.
- [19] Patidar MK, Ranawat K, Matkawala F, Nigam S, Das AK. Polylactic acid blends: an insight to their microbial production, biodegradation and applications. *Environmental Sustainability*. 2024;7(4):439-59.
- [20] Srivastava A, Mishra A. Food waste valorization for handling environmental problems: a review. *Environmental Sustainability*. 2022;5(4):401-21.
- [21] Ali W, Das S, Thery J, Jeong H, Lee J-S, Zinck P, et al. Acute and multigenerational toxicity of polylactic acid microplastics on a copepod bioindicator. *Environmental Chemistry Letters*. 2024;22(5):2167-75.
- [22] Balakrishnan A, Appunni S, Chinthala M, Jacob MM, Vo D-VN, Reddy SS, et al. Chitosan-based beads as sustainable adsorbents for wastewater remediation: a review. *Environmental Chemistry Letters*. 2023;21(3):1881-905.
- [23] Elshabrawy SO, Elhady S, Elhussieny A, Dey T, Fahim IS. Preparation and characterization of face masks made of bagasse, starch and chitosan obtained from agricultural and food wastes. *Environmental Sustainability*. 2024;7(3):339-48.
- [24] Vijayaram S, Razafindralambo H, Sun Y-Z, Vasantharaj S, Ghafarifarsani H, Hoseinifar SH, et al. Applications of green synthesized metal nanoparticles—a review. *Biological Trace Element Research*. 2024;202(1):360-86.
- [25] Karami N, Mohammadpour A, Samaei MR, Amani AM, Dehghani M, Varma RS, et al. Green synthesis of sustainable magnetic nanoparticles Fe₃O₄ and Fe₃O₄-chitosan derived from *Prosopis farcta* biomass extract and their performance in the sorption of lead (II). *International Journal of Biological Macromolecules*. 2024;254:127663.
- [26] Duan Y-T, Soni K, Patel D, Choksi H, Sangani CB, Saeed WS, et al. Green synthesis of iron oxide nanoparticles using *Nicotiana glauca* and their biological evaluation. *Journal of Molecular Liquids*. 2024;396:123985.
- [27] Zafar S, Farooq A, Batool S, Tariq T, Hasan M, Mustafa G. Green synthesis of iron oxide nanoparticles for mitigation of chromium stress and anti-oxidative potential in *Triticum aestivum*. *Hybrid Advances*. 2024;5:100156.
- [28] Varaganti V, Vishnu A, Vedanth NP, Pusuluri RC, Panniru AC, Potluri S, et al. Microbes in regenerative medicine: a narrative review. *Regenerative Medicine Reports*. 2025:10.4103.
- [29] Poerio A, Petit C, Jehl J-P, Arab-Tehrany E, Mano JF, Cleymand F. Extraction and physicochemical characterization of chitin from cicada orni sloughs of the south-eastern French mediterranean basin. *Molecules*. 2020;25(11):2543.
- [30] Gholivand MB, Piryaei M, Maassoumi SM. Antioxidant activity of *Ziziphora tenuifolia* methanolic extracts and comparison of the essential oil in two stages of growth. *Chinese journal of natural medicines*. 2014;12(7):505-11.
- [31] Rafaathaghighi A, Jafari L, Mirzaalian Dastjerdi A, Abdollahi F. The Effect of Edible Coating with Alginate and Shirazi Thyme Essential Oil on the Qualitative Characteristics of Ber Fruit (*Ziziphus mauritiana* Lam.) during Storage. *Iranian Food Science and Technology Research Journal*. 2024;20(4):465-83.
- [32] Pena-Pereira F, Wojnowski W, Tobiszewski M. AGREE—Analytical GREENness metric approach and software. *Analytical chemistry*. 2020;92(14):10076-82.
- [33] Shen S, Qu X, Liu Y, Wang M, Zhou H, Xia H. Evaluation of Antioxidant Activity and Treatment of Eczema by Berberine Hydrochloride-Loaded Liposomes-in-Gel. *Molecules*. 2024;29(7):1566.
- [34] Benjamaa R, Elbouny H, Errati H, Moujanni A, Kaushik N, Gupta R, et al. Comparative evaluation of

- antioxidant activity, total phenolic content, anti-inflammatory, and antibacterial potential of Euphorbia-derived functional products. *Frontiers in Pharmacology*. 2024;15:1345340.
- [35] Piryaei M, Abolghasemi MM, Memari S. Three-dimensional ZnS/MoS₂ on cellulose paper for determination of Digoxin in urine and plasma. *Nanochemistry Research*. 2024;9(1):68-76.
- [36] Shoudho KN, Uddin S, Rumon MMH, Shakil MS. Influence of Physicochemical properties of Iron Oxide nanoparticles on their antibacterial activity. *ACS omega*. 2024;9(31):33303-34.